Downlink System Throughput Statistics for Various MEA Configurations

Rahul N. Pupala
Alcatel-Lucent/Bell Labs, Murray Hill, NJ 07974, USA
Email: rahul.pupala@alcatel-lucent.com

Yifei Yuan (*Senior Member, IEEE*)
ZTE Corporation, Morristown, NJ 07960, USA
Email: yifei.yuan@zteusa.com

Qi Bi (*Fellow, IEEE*)
China Telecom - Beijing Research Institute, Beijing, China
Email: qibi@ctbri.com.cn

Larry J. Greenstein (*Life Fellow, IEEE*)
ECE (WINLAB), Rutgers – The State University of New Jersey, North Brunswick, NJ 08902, USA
Email: ljg@winlab.rutgers.edu

***Abstract*— The advent of applications that need higher throughputs motivates wireless service providers and cellular operators to embrace newer technologies that can meet these demands. Multiple-input-multiple-output (MIMO) systems have shown promise in their ability to deliver high throughput per bandwidth with reasonable constellation sizes. Adding antennas at the base station (BS) is practical due to reasons of size and cost amortization over users. However, adding antennas at the mobile station (MS), which does not have similar advantages, needs to be carefully evaluated. We therefore consider the more general class of techniques involving a multiple-element antenna (MEA) at one or both ends of the link (MIMO corresponding to the case of both).**

From a commercial standpoint, one needs to address the following questions: (i) What is the benefit of a second antenna at the BS or the MS relative to the single-input-single-output (SISO) case? (ii) What is the added value of a second antenna at both ends? (iii) If a second antenna is indeed used at both ends, which mode of operation — spatial multiplexing (SM) or diversity (Div) — is the preferred one? Using (n, m) to denote a link with n BS transmit elements and m MS receive elements, we compare the downlink throughput performance of the SISO link with that of four MEA configurations: $(1, 2)$, $(2, 1)$, $(2, 2)$ with Div and $(2, 2)$ with SM. Our results indicate that, in the context of adaptive modulation with practical limits on constellation size, $(1, 2)$ is the preferred configuration. We also show this finding to be robust to assumptions used in the study.

***Index Terms*— SISO, MIMO, MEA, MMSE, multipath fading, shadow fading, co-channel interference, cross-stream interference, interference cancellers**

I. Introduction

Multiple-input-multiple-output (MIMO) systems have been accepted as a significant breakthrough in modern digital communications, due to their ability to deliver higher spectral efficiencies with reasonable constellation sizes, as compared to single-input-single-output (SISO) systems [1]–[3]. A laboratory implementation of the so-called vertical Bell Labs layered space time architecture (VBLAST) demonstrated the feasibility of the MIMO concept, delivering spectral efficiencies of 20–40 bps/Hz under indoor conditions [4]. Not surprisingly, MIMO's potential is being tapped for commercial wireless products and networks such as wireless local area networks (WLANS), third-generation (3G) cellular networks, WiMAX, and future Internet-intensive wireless networks (including 4G networks).

A multi-element antenna (MEA) link (of which MIMO is a special case) employs a multi-element array at one or both ends. When only one end of the link uses an MEA, diversity can be achieved; this improves quality and thus enables higher throughput via larger signal constellations. When *both* ends use an MEA — the MIMO case — it is possible to enhance throughput via either diversity (Div), as above; spatial multiplexing (SM), whereby the receiver can de-couple multiple parallel streams sent by the transmitter; or a combination of both [5].

We will study and compare the performance of SISO links and several kinds of MEA links. Application type determines which aspect of performance matters most. For some applications (e.g., data), higher throughput, even if over intermittent connections or over smaller separation distances will be deemed as "good", while other applications (e.g., voice, streaming) may prefer to trade throughput for sustained connections and/or a wider coverage area. It is thus clear that no single performance metric will suffice. Accordingly, we study the following metrics: (i) the mean, over the cell, of the per-link

Manuscript received February 15, 2011; revised May 15, 2011; accepted June 15, 2011.

doi:10.4304/jcm.6.4.285-292

TABLE I.
3GPP2 SIMULATION PARAMETER SUMMARY

1	Cell Geometry	Regular array of hexagonal cells, with site-to-site distance 2.5 km (i.e., cell radius of 1.4434 km).
2	Number of Cells	1 tier-ring, 3 sector system (21 sectors total).
3	Antenna Horizontal Pattern (sectoring)	70° (–3 dB), with 20-dB front-to-back ratio (see Note 1 below).
4	Antenna Orientation	0° azimuth is North (main lobe). No loss is assumed on the vertical dimension.
5	Propagation Model	$28.6 + 35\log_{10}(d)$ dB, d in meters. Modified Hata Urban Propagation Model @ 1.9 GHz (COST 231). Min. separation of 35 m between MS and BS.
6	Lognormal Shadowing	Standard Deviation $\sigma = 8.9$ dB (see Note 2 below).
7	Base Station Correlation	0.5 (see Note 2 below).
8	Mobile Noise Figure	10 dB.
9	Thermal Noise Density	-174 dBm/Hz.
10	Carrier Frequency	2 GHz.
11	System Bandwidth	5 MHz.
12	BS Antenna Gain	15 dB total from 17 dB BS gain; 2-dB cable loss.
13	Other Losses	10 dB.
14	Fast Fading Model	Rician (see Table 2).
15	BS maximum PA Power	20 W.
16	Maximum C/I achievable	13 dB for typical IS-95 and cdma2000 1x systems and 18 dB for 1xEV-DV and 1xEV-DO systems.

throughput and (ii) 30th percentile of the link throughput.

Mean throughput provides a measure of the *data volume* an operator can deliver, in that this quantity times the number of channels per cell is a good approximation to the total throughput per cell. The 30th percentile of throughput is a useful measure of *user perception*, in that the vast majority of users (70%) will experience this throughput or more. Each metric thus has value from one perspective or another.

The essential aim of this study is to decide the merit in modifying a SISO link with added antenna elements at one or both ends. We denote a general downlink configuration by (n, m), where n is the number of base station (BS) transmit elements and m is the number of mobile station (MS) receive elements. Considering present-day technology and economics, we limit our study to the possibility of at most two antenna elements at each end. Thus, we investigate five configurations in all: $(1, 1)$, which is SISO; $(2, 1)$, MISO with transmit diversity; $(1, 2)$, SIMO with minimum-mean-square-error (MMSE) receiver; $(2, 2)$ with Div; and $(2, 2)$ with SM. Computing the performances of these configurations, based on the metrics cited above, the differences can be used to decide whether (and where) addition of antenna elements is justified. By studying the performance of particular MEA configurations[1] for a specific standard (3GPP2), we are augmenting our knowledgebase in [6]–[9].

Systems engineers from several commercial companies have performed similar studies, for both High Speed Packet Access (HSPA) and Long Term Evolution (LTE) networks. Their contributions feed into the knowledge-base maintained by the standards bodies (3GPP, 3GPP2), and can be found in [10]. A sampling of academic investigations for MIMO capacities is [11]–[13]. The rest of this paper is organized as follows. We discuss the simulation platform in Section II, and the results in Section III. Section IV summarizes our work, and presents some key conclusions.

[1]For configuration $(1, 2)$, we can employ either the maximal ratio combiner (MRC) or the minimum mean square error (MMSE) receiver structure. Of the two, MMSE is higher performing, as it offers an optimal balance between diversity and co-channel interference suppression, leading to higher throughput. MRC on the other hand offers only a diversity benefit.

II. SIMULATION PLATFORM

We developed a system-level simulation platform for computing the throughputs of MEA cellular systems. The test bed is sufficiently general to allow us to work with several key system-level parameters, namely, size of the transmit and receive MEAs; frequency reuse factor; antenna pattern (omni or sectorized); degree of error protection (perfect coding, no coding, or intermediate coding strategies); maximum constellation size; and, Rician K-factor.

A. MIMO System Model

In our MIMO cellular data environment, a given cell, consisting of a serving BS and a MS on every frequency channel, is surrounded by one contiguous tier of six cells. Our platform incorporates aspects of the 3GPP2 environment, as detailed in Table I.

NOTES

1. The base station antenna pattern used for each sector, is specified by

$$G(\theta) = -\min\left[12\left(\frac{\theta}{\theta_{3\text{dB}}}\right)^2, A_m\right]\text{dB}, \ -180 \leq \theta \leq 180,$$

where $\theta_{3\text{dB}}$ is the 3-dB azimuth beamwidth and A_m = 20 dB is the maximum attenuation.

TABLE II.
VARIATION OF RICIAN K-FACTOR AS A FUNCTION OF BS-MS SEPARATION DISTANCE (PERCENTAGES SPECIFY THE DISTANCES RELATIVE TO THE CELL RADIUS).

Distance %	0-5	5-15	15-25	25-35	35-45	45-55	55-65	65-75	75-85	85-100
Rician K	10	9	8	7	6	5	4	3	2	0

2. The random shadow fading x_k between a MS and a BS$_k$ (whether serving or interfering) is the weighted sum of a component z common to all cell sites and a component z_k which is independent of z and from one cell site to the next. Both components are Gaussian distributed with zero mean and standard deviation σ. Thus, $x_k = az + bz_k,\ k = 0 \dots 6$, where $a^2 + b^2 = 1$. In this study, we assume $a^2 = b^2 = 1/2$, meaning that x_u and x_v, $u \neq v$, are 50% correlated.

The complex baseband channel gain between the jth transmit antenna and the ith receive antenna is modeled by

$$h_{ij} = \sqrt{G(\theta)}\sqrt{A\left(\frac{d_0}{d}\right)^{\Gamma} s}\left[\sqrt{\frac{K}{K+1}}e^{j\phi} + \sqrt{\frac{1}{K+1}}z_{ij}\right], \tag{1}$$

where

- θ is the angle between the 0° azimuth, and the BS-MS link.
- d is the link length, Γ is the path loss exponent, and A is the median path gain at reference distance d_0.
- $s = 10^{S/10}$ is a log-normal shadow fading variable, where S is a zero-mean Gaussian random variable with standard deviation σ dB.
- $\phi = 2\pi d/\lambda$ is the phase shift of a plane wave from the transmitter to the receiver. We assume that for a given transmit-receive pair, all link-paths have the same length.
- z_{ij} represents the phasor sum of scattering components for the (i, j) path. These are assumed to be zero-mean, unit-variance, i.i.d. complex Gaussian random variables.
- K is the Rician K-factor.

Using appropriate parameter values in (1), the path-loss portion of the channel gain formula (first square root term outside the brackets) is made to follow the propagation model specified in Table I (Item 5). The Rician K-factor typically decreases as the MS moves farther away from the BS. The assumed variation of the K-factor with distance is given in Table II.

B. System Model Assumptions

We invoke the assumptions often made in conjunction with MIMO systems [1], [3]: (i) narrowband signaling, (ii) quasi-static (block) fading, (iii) long burst interval, and (iv) independently faded Rayleigh/Rician path gains. This permits a mathematical representation for the MIMO cellular system as follows:

$$\mathbf{Y} = \mathbf{H}\mathbf{X} + \mathbf{Z}, \tag{2}$$

where $\mathbf{X} \in \mathbb{C}^{7n}, \mathbf{Y} \in \mathbb{C}^{m}$, are transmit (serving and interfering) and receive signals, $\mathbf{H} \in \mathbb{C}^{m\times 7n}$ is the channel gain and $\mathbf{Z} \in \mathbb{C}^{m}$ is thermal noise, that is Gaussian distributed with zero mean and power spectral density (PSD) N_0. Since the noises corrupting the different receive antennas are independent, $\mathbf{Z}$ has an autocorrelation matrix $N_0\mathbf{I}_{m\times m}$, with $\mathbf{I}_{m\times m}$ being the identity matrix.

We assume only one tier of interferers around the serving BS. This assumption is made to simplify the simulations and is slightly optimistic; however, the rapid decay of signal power with distance makes this assumption reasonable. Moreover, we offset it with the pessimistic assumption that all co-channel interferers are transmitting all the time.

We assume an algorithm that perfectly adapts the transmission (via the constellation size[2]) according to the instantaneous radio channel and interference conditions. For $(2, 2)$ SM, it is possible for different transmit antennas to choose different constellation sizes.

The transmit power per antenna element is P/n so that the total power transmitted on each link is the same regardless of n. Additionally, since cell-site (macro) diversity has been shown to have minimal impact on mean throughput calculations [14], [15], we do not use this in our simulations, i.e., for simplicity, we assume that users communicate with the base station that is the nearest, not necessarily strongest.

C. Array Processing Schemes

1) Transmit Diversity via Alamouti Coding: The Alamouti scheme is an optimal transmit diversity scheme. It is optimal in the sense that it offers the maximum code rate ($r = 1$) and does not suffer from any loss of performance as compared to an MRC diversity scheme [16], [17]. Specific engineering aspects of this scheme are detailed in [18].

Under the assumption that noise plus co-channel interference (CCI) can be treated as complex Gaussian, the Alamouti scheme on a $(2, m)$ link has the same performance as the $(1, 2m)$ MRC receiver at half the transmit power of the $(2, m)$ MIMO configuration [18]. This enables an easy computation of the signal-to-interference-plus-noise-ratios (SINRs):

$$\gamma_i = \frac{|h_{i0}|^2(P/2)}{\sigma^2 + \sum_k \mathrm{CCI}_{ik}}, \quad i = 1, 2, \dots, 2m, \tag{3}$$

$$\gamma_{\text{alamouti}} = \sum_i \gamma_i, \quad i = 1, 2, \dots, 2m, \tag{4}$$

[2]The procedure to compute the optimum size of the transmit constellations for all five configurations will be made explicit later (see Appendix).

TABLE III.
OFFSETS FROM THE SHANNON CURVE FOR THE CONFIGURATIONS UNDER CONSIDERATION.

Configuration	$(1,1)$ SISO	$(2,1)$ Div	$(1,2)$ MMSE	$(2,2)$ Div	$(2,2)$ SM
Offset (dB)	3.5	4	4	5	6

where:

- h_{i0} is the instantaneous signal gain from the serving BS to the ith receive antenna.
- P is the total transmitter power.
- CCI_{ik} is the instantaneous power from the kth interfering BS at the ith receive antenna.
- γ_i is the input SINR at the ith branch of the MRC receiver.
- $\gamma_{alamouti}$ is the SINR at the receiver output.

Equation (4) is the well known result that the SINR of an MRC receiver is equal to the sum of SINRs of its individual branches.

2) The Minimum Mean-Square Error (MMSE) Receiver: MIMO permits the creation of several parallel transmission streams, i.e., spatial multiplexing. These streams interfere at each receive antenna, which the receiver array processor separates by using an appropriate set of weights. In this study, we assume use of the MMSE processor to implement spatial de-multiplexing. Other possible receiver array processors are zero-forcing (ZF), successive-interference-cancellation (SIC), ordered-SIC (OSIC) and OSIC-MMSE [14].

The MMSE array processing scheme separates the received signals by computing a linear combination of the received signals using a set of weights that achieves the minimum mean-square error between the output estimate and the true signal sample. Thus,

$$\hat{\mathbf{X}} = \mathbf{W}^H \mathbf{Y}. \tag{5}$$

The performance index is,

$$\zeta(\mathbf{W}^H) \triangleq E\left[\sum_{j=1}^{n} |\epsilon_j|^2\right] = E\left[\sum_{j=1}^{n} |x_j - \hat{x}_j|^2\right], \tag{6}$$

where x_j is the jth transmitted signal. The expectation in (6) is taken with respect to the noise and the statistics of the data sequences. The desired weight matrix that yields the minimum mean square error is given as [14]

$$\mathbf{W} = \mathbf{A}^{-1}\mathbf{H}, \tag{7}$$

where,

$$\mathbf{A} = \mathbf{H}\mathbf{H}^H + \frac{\sigma^2}{P/n}\mathbf{I}_{m\times m}. \tag{8}$$

The post-processing SINR on the jth decoded stream can be shown to be [14], [19],

$$\gamma_j = (\mathbf{H})_j^H \mathbf{R}_j^{-1} (\mathbf{H})_j, \quad j = 1, 2, \ldots, n, \tag{9}$$

where

$$\mathbf{R}_j = \sum_{l=1,\ l\neq j}^{7n} (\mathbf{H})_l (\mathbf{H})_l^H + \frac{\sigma^2}{P/n}\mathbf{I}_{m\times m}, \tag{10}$$

and $(\mathbf{H})_j$ is the jth column of $\mathbf{H}$.

D. Link Throughput

For AWGN channels, achievable throughput is upper-bounded by the Shannon limit

$$T_j = \log_2(1 + \gamma_j), \tag{11}$$

where T_j is the sub-channel throughput. The per-user data throughput is $\sum_j T_j$.

For practical systems, it is known that link throughput can be approximated by using curves shifted by SINR "offsets" from the Shannon curve [20]. The exact offset used depends on the link configuration (SISO, MEA), the receiver structure, etc. We can thus write

$$T_j = \log_2\left(1 + \frac{\gamma_j}{10^{x/10}}\right). \tag{12}$$

The authors in [20] report that a 3-dB offset from the Shannon curve is needed to take into account finite alphabets and imperfect channel coding (especially when the block size is not very large), and overhead. For the SISO configuration, the channel estimation SINR penalty — from the overhead of the pilot signals and from non-ideal demodulation using the noisy channel estimate — is about 0.5 dB. This leads to an overall 3.5-dB offset for the SISO configuration.

When two transmit antennas are employed, the transmit power of the pilot has to be split evenly between them; and when two receive antennas are employed, the operating point of each receive antenna is lowered by 3 dB. In either case, the channel estimation penalty gets worse by about 0.5 dB as compared to SISO. When two transmit and two receive antennas are employed, the offset used is 1.5 dB — which is more than the cumulative effect of using either two transmit antennas or two receive antennas. Moreover, in $(2,2)$ SM, there is an additional 1-dB penalty in channel estimation, since the MMSE receiver needs to invert the channel gain matrix as part of the channel estimation procedure. This leads to the offsets from the Shannon curve, Table III.

We will use these SINR offsets in our computations. To confirm the robustness of our conclusions, however, we will also consider the case where all offsets are the same, as we discuss next.

III. SIMULATION RESULTS

We computed throughputs of all five configurations cited above, both where the SINR offsets are non-uniform, as given by Table III, and where they are all the same. In the latter case, we use a 6-dB offset.

TABLE IV.
MEAN THROUGHPUT OBTAINED FOR THE VARIOUS CONFIGURATIONS.

System	$(1, 1)$ SISO	$(2, 1)$ Div	$(1, 2)$ MMSE	$(2, 2)$ Div	$(2, 2)$ SM
Diff. Est. Offsets (bps/Hz)	2.50	2.58	3.17	2.87	3.06
Unif. Est. Offsets (bps/Hz)	2.24	2.37	3.00	2.77	3.06

TABLE V.
30TH PERCENTILES OF THE MULTIPATH-AVERAGED THROUGHPUTS OBTAINED FOR THE VARIOUS CONFIGURATIONS.

System	$(1, 1)$ SISO	$(2, 1)$ Div	$(1, 2)$ MMSE	$(2, 2)$ Div	$(2, 2)$ SM
Diff. Est. Offsets (bps/Hz)	0.64	0.66	1.60	0.97	0.52
Unif. Est. Offsets (bps/Hz)	0.43	0.47	1.26	0.83	0.52

Trying many possible combinations of offsets for the various configurations is too expensive an undertaking for gauging the sensitivity of conclusions to the chosen SINR-offsets. The search space is considerably reduced by investigating reasonable offsets that will likely "stress test" our conclusions. This is best brought about by using offset values that benefit the $(2, 2)$ configurations or degrade the performance of the others. A uniform 6-dB offset for all configurations is one such example.

For the purpose of averaging, we distribute the MS with uniform randomness at 1000 locations over a given sector. To accommodate the fact that shadow fading and multipath fading are random, we allow each MS to experience 100 different shadow fades at a given location, and 1000 different multipath fades for each location-shadowing combination.

In this study, we permit only a small, discrete set of constellation sizes — BPSK and $4/8/16$-QAM (corresponding, respectively, to symbol rates of $1/2/3/4$ bits/symbol). These sizes are practical for present-day implementations. We now address the main questions motivating this study:
(i) What is the benefit of a second antenna at the BS or MS relative to the SISO case?
(ii) What is the added value of a second antenna at both ends?
(iii) If a second antenna is indeed used at both ends, thereby creating a MIMO $(2, 2)$ system, which mode of operation — SM or Div — is the preferred one?

We shall answer these questions by measuring how each configuration fares for each metric defined earlier. Our results are summarized next.

A. Metric 1: Mean Throughput

This metric gives the average of the link throughput, Table IV.

From this table, we conclude the following:

- $(1, 2)$ MMSE is the best configuration for the case of differential SINR-offsets, and is very close to the best configuration for the case of uniform SINR-offsets. Hence neither $(2, 2)$ configuration is attractive, considering receiver complexity and costs.
- $(2, 1)$ Div is only slightly better than $(1, 1)$, and is within approximately 0.6 bps/Hz of (1, 2) MMSE.
- $(2, 2)$ SM is slightly better than $(2, 2)$ Div.
- The performance gap among configurations narrows for the more realistic case of differential offsets as compared to the case of uniform offsets.

B. Metric 2: 30th Percentile of User Throughputs Cell-Wide

This metric gives the throughput achieved or exceeded on 70% of all links, taken over location and fading state, Table V. From this table, we draw conclusions similar to those above except that in this case $(2, 2)$ Div fares slightly better than $(2, 2)$ SM.

$(2, 2)$ SM produces lower multipath-averaged throughputs for its 30th percentile users than $(2, 2)$ Div (Table V), but produces higher mean throughput (Table IV). Since both configurations see the same set of users statistically, it is the receiver structure that results in the creation of these differences. The implication is that stream decoupling/cross-stream interference (XSI) in SM works against some set of users, while enhancing a favored set of users. Div, on the other hand, attempts throughput improvement over all users. These differences will likely further exaggerate for higher-order MEAs.

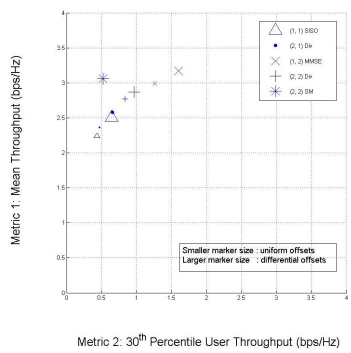

Figure 1. Scatter plot of the five configurations for Metrics 1 and 2. Both cases, uniform (smaller markers) and differential offsets (larger markers), are shown. For the $(2, 2)$ SM case, the values overlap (See the last column in Tables IV and V).

Fig. 1 shows a scatter plot ranking all five configurations for both Metrics 1 and 2. The plot enables us to see two perspectives simultaneously. From both perspectives, and for either offset case, $(1, 2)$ MMSE is more attractive than the others, confirming previous conclusions.

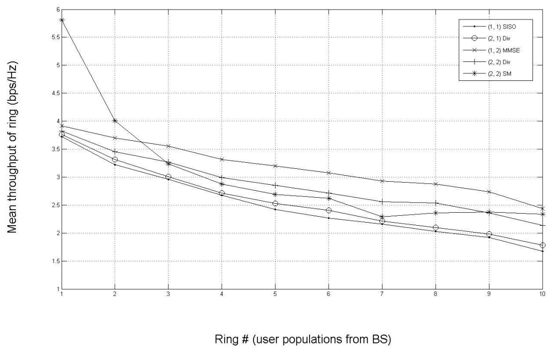

Figure 2. Mean throughputs of 10 rings of equal user population with differential SINR offsets.

Fig. 2 shows the mean throughputs of 10 concentric rings of equal user population. Ring 1 consists of the 10% of users closest to the BS. The throughput is averaged over multipath fading, shadowing, and location (the users in the ring). Examining Fig. 2, we see that:

- For users closest to the BS, $(2, 2)$ SM offers a high average throughput.
- For other users, all configurations except $(1, 2)$ MMSE provide comparable performance, with $(2, 2)$ SM doing slightly better than $(2, 2)$ Div for ring 10.

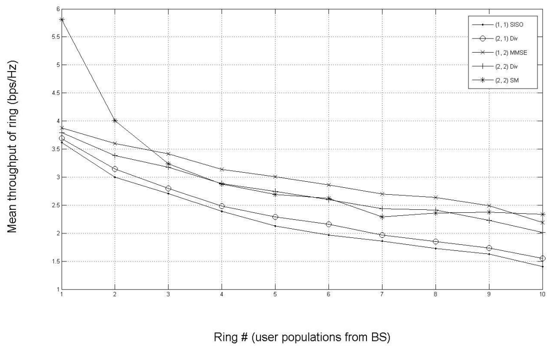

Figure 3. Mean throughputs of 10 rings of equal user population with uniform SINR offsets.

Fig. 3 shows the same plot for the case of uniform SINR-offsets. As expected, the curves diverge, since higher-order MEAs benefit from a lower relative offset penalty. However, the divergence is small. Moreover, except for populations closest to the BS, $(1, 2)$ MMSE remains the most attractive configuration.

We have established that, although both SINR-offset cases result in minor differences in throughputs of the configurations, they do not change the overall conclusions. Therefore, we drop the case of uniform SINR-offsets from further consideration, opting to use the more realistic case of differential SINR-offsets from this point on.

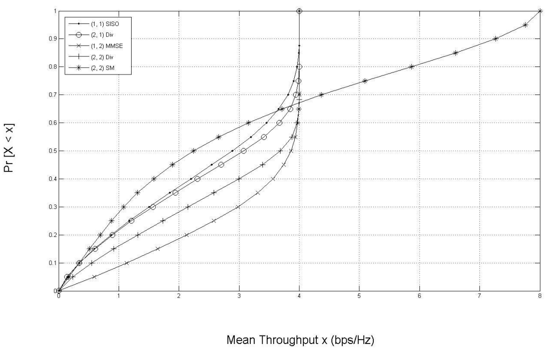

Figure 4. Fast-fading-averaged cell-wide distribution of throughput for all five configurations (differential offsets).

Fig. 4 shows another throughput statistic: the distribution of multipath-averaged user throughputs on a cell-wide basis. The following salient points should be noted:

- All configurations, with the exception of $(2, 2)$ SM, operate with only one transmit stream and hence have a peak rate of 4 bps/Hz. $(2, 2)$ SM operates with two streams, thus it can offer up to 8 bps/Hz.
- $(2, 2)$ SM appears lucrative only for throughput requirements exceeding 4 bps/Hz. In fact, for throughputs less than 4 bps/Hz, it is the worst configuration.
- In the mid-region, the curves are about parallel to one another. It is for this reason that the value of the percentile chosen (lowest 30th) for Metric 2 is arbitrary.

IV. Summary and Conclusions

The objective of this study was to quantify and compare the throughput performance of five link configurations involving one or two antenna elements at each end.

Our results indicate that, in the context of a limited number of constellation sizes, and for the case of differential SINR-offsets, $(1, 2)$ MMSE is the configuration of choice for both metrics considered. The other four are comparable in performance with each other. The main reasons why $(1, 2)$ MMSE scores best are: relatively low channel estimation penalty, the absence of cross-stream interference at receive antennas, and an excess receive antenna to suppress CCI.

For the case of uniform offsets, the throughput results change by small amounts, but the main conclusions do not change from those for differential offsets. This reinforces our findings and shows them to be robust to assumptions used in the study.

The MMSE receiver assumed here for $(2, 2)$ SM is one example of the many receivers that can decouple the SM streams; ZF, SIC, OSIC, and OSIC-MMSE receivers are some others. Since changing the particular receiver amounts to changing the SINR offset, against which our conclusions are found to be stable, we claim that $(1, 2)$ MMSE is the preferred configuration regardless of the particular receiver chosen by $(2, 2)$ SM to de-couple its streams.

Appendix A Project Description Summary

It is clear that we intend to compute throughput statistics of the five configurations. For the benefit of the reader, we list the steps involved:

- Distribute MSs in cell.
- Generate channel matrix $\mathbf{H}$ as given by (1). The size of $\mathbf{H}$ is given by (2).
- Compute post-processing SINR of substream j [(3) and (4) for Div, (9) and (10) for SISO, MMSE and SM].
- Compute throughputs for substream j [(12) and Table III].
- The "MEA throughput" is sum of the throughputs of the individual substreams.

At the beginning of each block-fade interval, pilot signals are transmitted to estimate the receiver array weights. The receiver then determines the constellation size (M) from the substream post-processing SINRs, and communicates this information to the transmitter. Adaptive modulations at each transmit antenna then quickly select the corresponding optimal QAM constellation. The channel remains known throughout, since estimation-feedback-adaptation occurs within the block fade interval.

Acknowledgement

We greatly appreciate valuable comments from Dennis Morgan (Bell-Labs, Murray Hill, NJ), Chandrasekharan Raman, Joydeep Acharya, Jasvinder Singh and David Daut.

References

[1] I. Telatar, "Capacity of multi-antenna gaussian channels," *Euro. Trans. Telecommun.*, vol. 10, no. 6, pp. 585–595, November 1999.

[2] G. Foschini and M. Gans, "On limits of wireless communications in a fading environment when using multiple antennas," *IEEE Wireless Personal Communications*, vol. 6, no. 3, pp. 311–335, March 1998.

[3] A. Paulraj, R. Nabar, and D. Gore, *Introduction to Space-Time Wireless Communications*. Cambridge University Press, 2003.

[4] P. Wolniansky, G. Foschini, G. Golden, and R. Valenzuela, "V-BLAST: an architecture for achieving very high data rates over the rich-scattering wireless channel," *in Proc. Int. Symp. Signals, Systems, and Electronics (ISSSE '98),* Pisa, Italy, pp. 295–300, October 1998.

[5] L. Zheng and D. Tse, "Diversity and multiplexing: a fundamental tradeoff in multiple-antenna channels," *IEEE Trans. Inf. Theory*, vol. 49, no. 5, pp. 1073–1096, May 2003.

[6] R. Pupala, L. Greenstein, and D. Daut, "Downlink throughput statistics in interference-limited cellular systems with multi-element antennas," *IEEE Trans. Commun.*, vol. 58, no. 1, pp. 311–317, January 2010.

[7] ——, "Throughput analysis of interference-limited MIMO-based cellular systems," *IEEE Trans. Wireless Commun.*, vol. 9, no. 6, pp. 1946–1951, June 2010.

[8] ——, "Effects of channel dispersion and path correlations on system-wide throughput in MIMO-based cellular systems," *IEEE Trans. Wireless Commun.*, vol. 8, no. 11, pp. 5477–5482, November 2009.

[9] R. Pupala, "Investigation of co-channel interference, channel dispersion & multiuser diversity in mimo-based cellular systems," Ph.D. dissertation, Rutgers - The State University of New Jersey, US, February 2008.

[10] "3GPP Standards Methodology Document 36.814."

[11] D. Gesbert, H. Bolcskei, D. Gore, and A. Paulraj, "MIMO wireless channels: capacity and performance prediction," *IEEE Proc. Globecom.*, pp. 1083–1088, Nov 2000.

[12] H. Sampath, S. Talwar, J. Tellado, V. Erceg, and A. Paulraj, "A fourth generation MIMO-OFDM broadband wireless system: design, performance, and field trial results," *IEEE Commun. Mag.*, vol. 40, no. 9, pp. 143–149, September 2002.

[13] F. Farrokhi, A. Lozano, G. Foschini, and R. Valenzuela, "Spectral efficiency of wireless systems with multiple transmit and receive antennas," *Proc. IEEE Symp. PIMRC*, vol. 1, pp. 373–377, September 2000.

[14] S. Catreux, "Techniques d' antennes multi-entrees multi-sorties dans un systeme de type cellulaire," Ph.D. dissertation, INSA, Paris, France, April 2000.

[15] S. Catreux, P. Driessen, and L. Greenstein, "Attainable throughput of an interference-limited multiple-input multiple-output (MIMO) cellular system," *IEEE Trans. Commun.*, vol. 49, no. 8, pp. 1307–1311, August 2001.

[16] V. Tarokh, H. Jafarkhani, and A. Calderbank, "Space-time block codes from orthogonal designs," *IEEE Trans. Inf. Theory*, vol. 45, no. 5, pp. 1456–1467, July 1999.

[17] V. Tarokh, N. Seshadri, and A. Calderbank, "Space-time block codes for high data rate wireless communication: Performance, criterion and code construction," *IEEE Trans. Inf. Theory*, vol. 44, no. 2, pp. 744–765, March 1998.

[18] S. Alamouti, "A simple transmit diversity technique for wireless communications," *IEEE J. Sel. Areas Commun.*, vol. 16, no. 8, pp. 1451–1458, October 1998.

[19] S. Catreux, L. Greenstein, and V. Erceg, "Some results and insights on the performance gains of MIMO systems," *IEEE J. Sel. Areas Commun.*, vol. 21, no. 5, pp. 839–847, June 2003.

[20] Q. Bi, S. Vitebsky, Y. Yang, and Y. Yuan, "Broadcast-multicast in 1x EV-DO revision a systems and its application to enhanced mobile services," *Bell-Labs Tech. J. (BLTJ)*, vol. 11, no. 4, pp. 237–252, December 2006.

Rahul N. Pupala received the B.E. degree in Computer Engineering from Victoria Jubilee Technical Institute (VJTI), Bombay in 1994, the M.S. degree in Computer Science in 2003, and the Ph.D. in Electrical Engineering in 2008 both from Rutgers - The State University of New Jersey. From 1994 to 1999, he worked in the software industry. He is currently at Alcatel-Lucent/Bell Labs, Murray Hill, NJ, responsible for PHY & MAC layer innovations for LTE-Advanced.

His research interests include Distributed Computing, Computer Networks, Signal Processing and Wireless Communications.

Yifei Yuan received Bachelor and Master degrees from Tsinghua University of China, and a Ph.D. from Carnegie Mellon University in 2000. He was with Alcatel-Lucent (formerly Lucent Technologies) from 2000 to 2008, working on intelligent antennas, advanced receiver, and channel element design for 3G and 4G wireless systems. Since 2008, he has been with ZTE, responsible for standards research on physical layer of LTE-Advanced. His research interests include multi-antenna technology, turbo codes, radio resource management.

Qi Bi received his M.S. from Shanghai Jiao Tong University in 1981 and Ph.D. from Pennsylvania State University in 1986. He was with Bell Laboratories for 20 years as a member of technical staff, then distinguished member of technical staff, senior manager and director. Since 2010, he has been the president of China Telecom Technology Innovation Center.

Dr. Bi has been active in technical conferences. He organized the first and the second CDMA conferences at Lucent Technologies in 1999 and 2000 and served as the technical chair for IEEE Globecoms wireless program from 2000 to 2002. He was the technical chair for the IEEE Wireless Communications and Network Conference in 2003. In 2005 and 2006, he serves as chair and organizer for the Wireless and Optical Communications Conference.

Dr. Bi was recognized in wireless areas. He received Awards of Excellence from the Advanced Technology Lab of AT&T in 1996 and 1997, and Bell Labs Presidents Gold Awards in 2000 and 2002. His team was awarded the Bell Labs Innovation Team Award in 2003 by the Bell Labs Basic Research Labs. In 2002, he became the first Chinese from the Peoples Republic of China to receive the prestigious Bell Laboratories Fellow Award. In 2005, he was recognized by the Chinese Institute of Engineers and was awarded the Asian American Engineer of the Year Award.

Dr. Bi has published extensively. He was also granted 35 US patents and 57 European patents. He is a Fellow of IEEE.

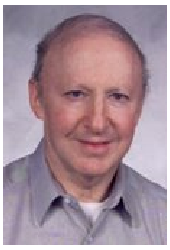

Larry J. Greenstein received the BS, MS and PhD degrees in electrical engineering from Illinois Institute of Technology in 1958, 1961 and 1967, respectively. From 1958 to 1970, he was at IIT Research Institute, where he worked on radio frequency interference and anti-clutter airborne radar. He joined Bell Laboratories in Holmdel, NJ in 1970. Over a 32-year career, he conducted research in digital satellites, point-to-point digital radio, optical transmission techniques and wireless communications. For 21 years during that period (1979-2000), he led a research department renowned for its contributions in these fields. Since 2002, he has been a research professor at Rutgers University's WINLAB, working on PHY-based security techniques, MIMO-based cellular systems, broadband power line systems, cognitive radio and channel modeling.

Dr. Greenstein is an IEEE Life Fellow, an AT&T Fellow, a recipient of the IEEE Communications Society's Edwin Howard Armstrong and Joseph LoCicero Awards, and co-author of several award-winning papers, including the IEEE Donald G. Fink Prize Paper Award. He has served on numerous editorial boards and technical program committees and was, and is now again, the IEEE Communications Society's Director of Journals.